Electrochemical and Solid-State Letters, **11** (4) G15-G18 (2008)
1099-0062/2008/11(4)/G15/4/$23.00 © The Electrochemical Society

Rapid Intergranular Corrosion of Copper in Sulfide-Polluted Salt Water

F. M. Al Kharafi, I. M. Ghayad, and B. G. Ateya*,z

Department of Chemistry, Faculty of Science, Kuwait University, Kuwait

Sulfide-induced intergranular corrosion (IGC) of copper was documented in salt water under free corrosion or controlled potential. The process was promoted by the oxidizing potential and the sulfide ions. A transition potential, E_t, of about −0.15 V (Ag/AgCl) was identified in the polarization curves in the presence of sulfide ions. Above E_t, sulfide ions accelerate IGC while having a modest effect on the rate of copper dissolution. Below E_t, they promote copper dissolution, while IGC occurs much more slowly. Various sulfur species were detected in the corrosion product using X-ray photoelectron spectroscopy.
© 2008 The Electrochemical Society. [DOI: 10.1149/1.2832428] All rights reserved.

Manuscript submitted October 31, 2007; revised manuscript received December 11, 2007.
Available electronically January 28, 2008.

Copper and many of its alloys have favorable combinations of mechanical, thermal, and electrical properties. Hence, they are manufactured in various forms and utilized in many industries, particularly in marine environments. The corrosion of copper and many of its alloys in such environments has been extensively studied.[1-7] These studies have primarily focused on characterization of the corrosion products and analysis of the results in terms of general corrosion. The stability of copper and its alloys in such an environment is attributed to the formation of a protective film of corrosion products which contains Cu_2O, $Cu_2(OH)_3Cl$, and other products.[1-7]

Among the various forms of corrosion of copper and its alloys, intergranular corrosion (IGC) has often received less attention. IGC has been recently linked to stress corrosion cracking of copper,[8,9] the failure of turbo-disks[10] and a gas inlet system in a petrochemical plant,[11] the structural degradation in turbine blades,[12] and fissures observed in AA7178 alloy during service in structural aircraft applications.[13] IGC has also been shown to cause failure of CuNi alloys in sea water.[3] The occurrence of IGC was also seen in bronze monuments in the Mediterranean basin.[14]

It is now widely recognized that many natural water bodies and industrial water streams are polluted with hydrogen sulfide. The literature has ample evidence for a promoting effect of sulfide ions on the corrosion of copper and its alloys.[15-25] This paper documents the occurrence of sulfide-induced IGC of copper in salt water. The process is shown to be rapid, being discernible within some tens of minutes. The present results are immediately relevant to the discussion of the proposed use of copper canisters for the disposal of Swedish, Finnish, and Canadian high-level nuclear waste deep in granite environment,[26] the rapid failure of copper nickel condenser tubes in wet hydrogen sulfide atmosphere,[27] and the microbiologically induced corrosion of Cu30Ni in anaerobic sea water.[28]

Experimental

Electrodes were prepared from electrolytic copper (99.9%) in the form of rods 0.96 cm in diameter. The working electrode was the cross-sectional area of the rod, and the immersed length of the rod was coated with a protective adhesive so that only the cross-sectional area was exposed to the solution. Electrical contact to the external circuit was made through the rod. The working electrodes were polished using SiC papers successively down to 2400 grits, followed by 0.3 micrometer alumina to acquire a mirrorlike finish. A conventional three-electrode cell was used with a Ag/AgCl reference electrode, $E = 0.197$ V SHE, and a Pt sheet counter electrode. Solutions were prepared using deionized water, AnalaR Na_2S, and NaCl from Fluka. Measurements were performed at 25 ± 1°C in 3.5 wt % NaCl solution. The surfaces of the electrodes were examined using an AXIO Imager A1M optical microscope, a JSM-6300 JEOL scanning electron microscope (SEM), and a VG Scientific 200 X-ray photoelectron spectrometer (UK), using Mg Kα radiation (1253.6 eV) operating at 13 kV and 23 mA. All measurements were performed while the solutions were open to air and were stirred using a magnetic stirrer.

Results

Polarization curves.— Figure 1 illustrates the effect of 10^{-3} M sulfide ions on the polarization curve of copper in the salt solution measured at a scanning rate of 5 mV s^{-1}. Sulfide ions shift the free-corrosion potential in the active direction by some hundreds of millivolts, which supports the findings of Rahmouni et al.[29] The polarization curve in the sulfide-polluted salt water can be divided into two regions, on either side of a transition potential (E_t) of about −0.15 V (Ag/AgCl). This transition potential marks a change in the effect of sulfide ions on the rate of copper dissolution. Below E_t, sulfide ions have a strong promoting effect on the rate of metal dissolution. Above this potential, sulfide ions have no significant effect on the rate of metal dissolution. However, as shown below, this is the region where sulfide ions have a marked effect on IGC of copper.

Current transients.— The copper surface was held under various potentials in the absence and in the presence of sulfide ions while the current transients were recorded. Figure 2 illustrates some of these results. Curves a and b refer, respectively, to the absence and presence of 10^{-3} M HS^- ions at a potential of −0.2 V (Ag/AgCl), which is below the transition potential, E_t. Note the marked effect of

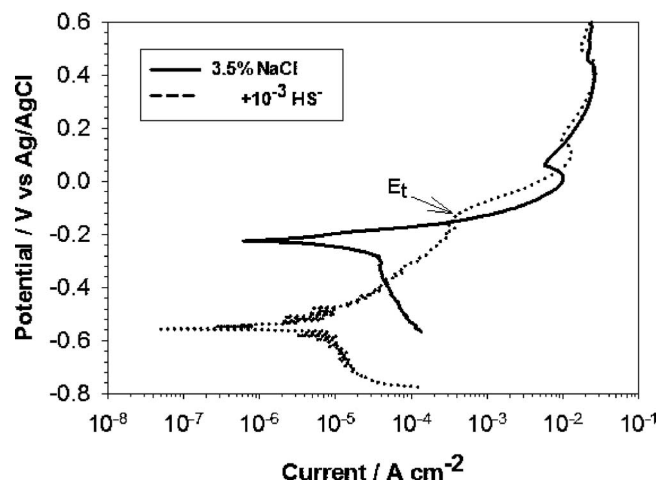

Figure 1. Effect of sulfide ions on the polarization curves of copper in 3.5% NaCl at 25°C. Note the transition potential, E_t, in the presence of sulfide ions.

* Electrochemical Society Active Member.
z E-mail: bgateya@yahoo.com

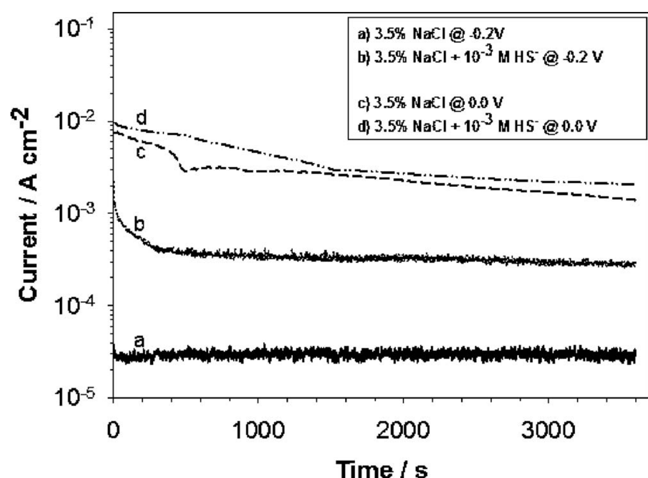

Figure 2. Effect of sulfide ions and electrode potential on the current transients of copper in the salt solution.

sulfide ions on the rate of metal dissolution. The presence of 10^{-3} M HS^- increases the rate of copper dissolution by about an order of magnitude. Curves c and d show the corresponding results at a potential of 0.0 V (Ag/AgCl), which is above the transition potential, E_t, where sulfide ions show only a modest effect on the rate of metal dissolution.

Scanning electron microscopy.— Figure 3 shows SEM images of copper surfaces potentiostated in 3.5% NaCl for 1 h at 0 V (Ag/AgCl) in the absence and in the presence of 10^{-3} M sulfide ions. Figure 3a shows the morphology of the surface that was corroded for 1 h in the salt solution in the absence of sulfide ions. Note the moderate general etching of the surface in the absence of sulfide ions. In the presence of sulfide ions, Fig. 3b, much more extensive corrosion appears with visible grain-boundary attack. A closer look at the topography of the corroded surface is given in Fig. 3c at a greater magnification, which shows the intersection of three grains. It reveals extensive corrosion on the grain surfaces in addition to the grain-boundary attack.

IGC of copper was also observed under free-corrosion conditions [about −0.5 V (Ag/AgCl)] after much longer times, compared to the case at 0.0 V (Ag/AgCl). Figure 4 shows an image of a copper surface that was kept under free-corrosion conditions for 24 h in the presence of 10^{-3} M sulfide ions. The figure clearly shows IGC in addition to corrosion on the grain surfaces. However, a much lower extent of corrosion is observed at the grain boundary and on the grain surface than that seen under the higher potential (see Fig. 3).

Characterization of corrosion products.— The corrosion products were characterized using energy-dispersive X-ray spectroscopy (EDS) and X-ray photoelectron spectroscopy (XPS). While EDS can be performed on selected regions of the corroded surface (on the scale of micrometers), it requires a fairly thick layer (of the order of micrometers) to be able to detect the presence of a certain element, with no indication of its oxidation state. XPS can detect as little as several atom layers of a certain element and can reveal its oxidation state. However, the XPS technique cannot be performed on selected regions, and hence it samples the entire surface.

EDS and XPS measurements were performed on samples corroded in the presence of sulfide ions. EDS results were obtained from regions inside and outside the grain boundaries under free-corrosion conditions and under a controlled potential of 0.0 V (Ag/AgCl). Figure 5 is an illustrative EDS spectrum of measurements obtained under all conditions. No sulfur signal was detected in the EDS spectra under any of the above conditions. However, the XPS spectra showed interesting sulfur signals. Figure 6a and b illustrate parts of the XPS spectra obtained from the copper surface that was corroded in the presence of 10^{-3} M HS^-, under free-corrosion conditions [about −0.5 V (Ag/AgCl)] and under 0.0 V (Ag/AgCl), respectively.

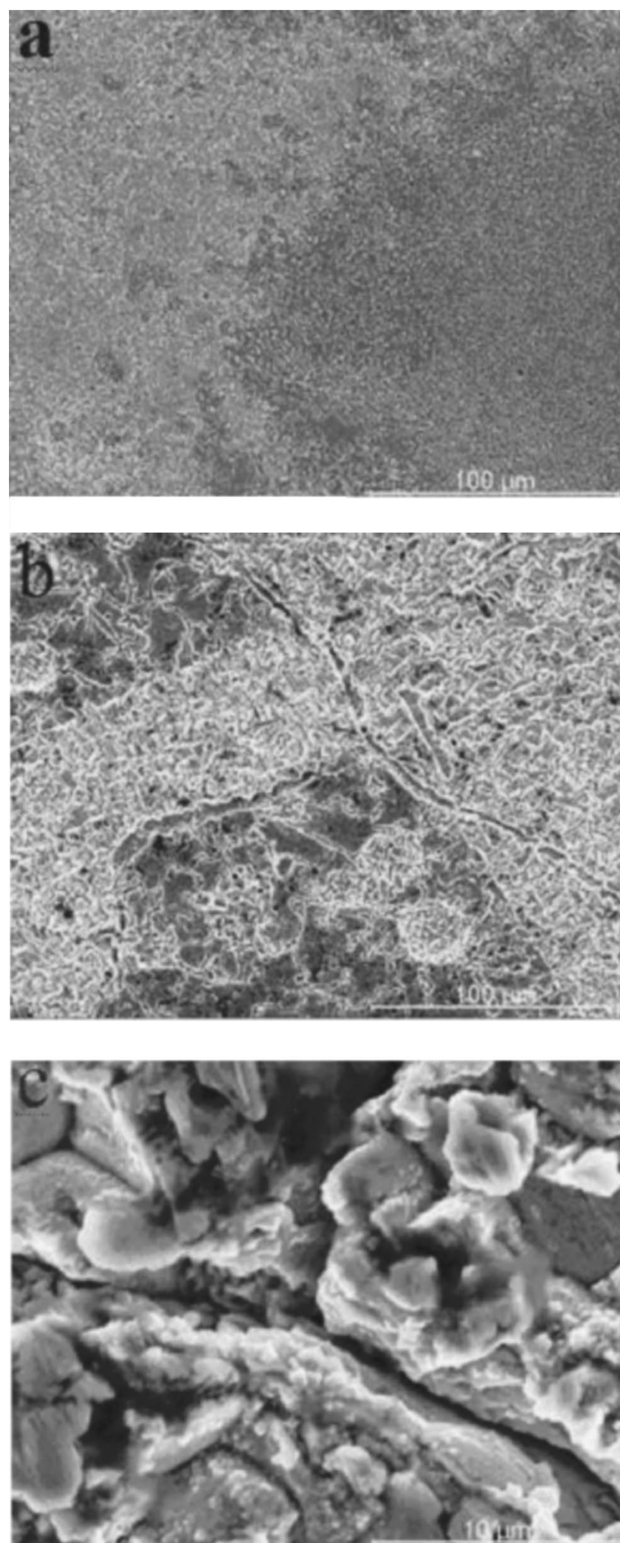

Figure 3. SEM image of copper treated under the following conditions: (a) potentiostated for 1 h at 0.0 V (Ag/AgCl) in 3.5% NaCl, (b) potentiostated for 1 h at 0.0 V (Ag/AgCl) in 3.5% NaCl + 10^{-3} M HS^-, and (c) intersection of three grains at higher magnification. Note the corrosion at the grain boundary and on the grain surface.

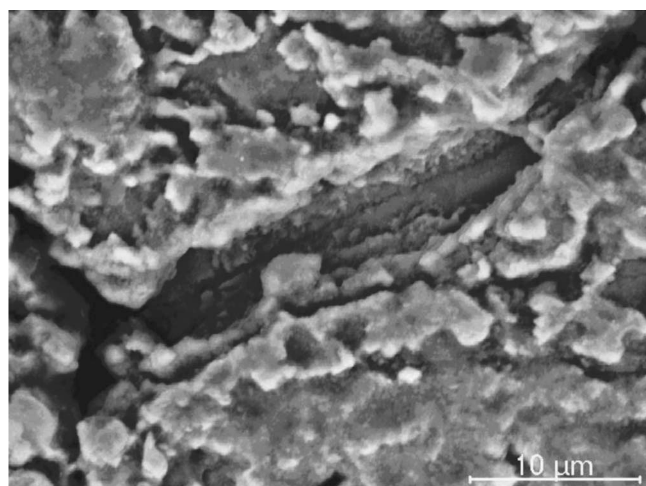

Figure 4. SEM micrograph of copper immersed for 24 h at the free-corrosion potential in 3.5% NaCl + 10^{-3} M HS^-.

The surface corroded under free corrosion shows a single S 2p peak at a binding energy of 162.0 eV (compared to C 1s at 248.6 eV). This is characteristic for copper sulfide.[7,30] The XPS spectrum of the surface that was corroded under the more noble potential of 0.0 V (Ag/AgCl) is much more complex. It reveals multiple composite peaks at binding energies of 162.0, 163.8, and 168.6 eV. These may be assigned, respectively, to sulfide ions, elemental sulfur, S_8, and sulfate.[7,30] This indicates that the sulfide ions oxidized under the noble potential of 0.0 V (Ag/AgCl) in addition to the formation of copper sulfide.

Discussion and Conclusions

The rate and mode of copper dissolution are clearly affected by the sulfide ions and the level of potential, as shown by Fig. 1-4. A transition potential, E_t, was observed only in the sulfide-polluted medium (Fig. 1). It marks a change in the effect of sulfide ions on the mode and rate of dissolution of copper. Below the transition potential, E_t, sulfide ions promote the dissolution of copper by virtue of increasing the magnitude of the anodic current at a certain potential. The process involves an adsorption step,[18,29] i.e.

$$HS^- + Cu = Cu{:}HS^- \qquad [1]$$

where $Cu{:}HS^-$ refers to an adsorbed HS^- ion on the copper surface. This adsorbed species is oxidized to give CuS, i.e.

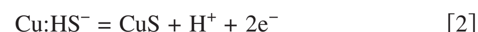

$$Cu{:}HS^- = CuS + H^+ + 2e^- \qquad [2]$$

Consequently, we see an increase in the rate of dissolution of copper at potentials below E_t, as shown in Fig. 1 and 2.

At potentials above E_t, IGC occurs quite rapidly in the sulfide-polluted medium. In this region, where the driving force for dissolution is quite high, sulfide ions have no marked effect on the rate of general metal dissolution. It follows that at these potentials, sulfide ions interact more strongly with the grain boundaries than with the grain surfaces. This reasoning is supported by the micrograph in Fig. 3c.

XPS spectra reveal some interesting findings about the role and fate of the sulfide ions. Thus, at the free-corrosion potential of about −0.5 V (Ag/AgCl), which is a fairly active value below E_t, the predominant sulfur species is sulfide ions at a binding energy of 162.0 eV. This can be easily rationalized in view of Eq. 2. At a potential of 0.0 V (Ag/AgCl), which is a fairly noble value above E_t, XPS spectra reveal the presence of sulfides, elemental sulfur S_8, and sulfate, SO_4^-. At such noble potentials, one expects the sulfide ions to undergo oxidation to give elemental sulfur and, eventually, sulfate[31,32]

$$HS^- \rightarrow S + H^+ + 2e \qquad [3]$$

$$HS^- + 4H_2O \rightarrow SO_4^- + 9H^+ + 8e \qquad [4]$$

These XPS findings are consistent with the results of a much more extensive study that was recently published on Cu30Ni.[7]

IGC of stainless steel has been attributed to chromium depletion at the grain boundaries, which results from the precipitation of chromium carbide.[33] The mechanism of IGC of copper has been much less studied or understood. The passivity of copper is attributed to the formation of a layer of Cu_2O which protects the underlying surface. It is also known that many impurities in copper segeregate to the grain-boundary region, such as Ni, Ag, Bi, Ta, As, P, etc.[34-39] Consequently, the oxide layer in the grain-boundary region is rich in

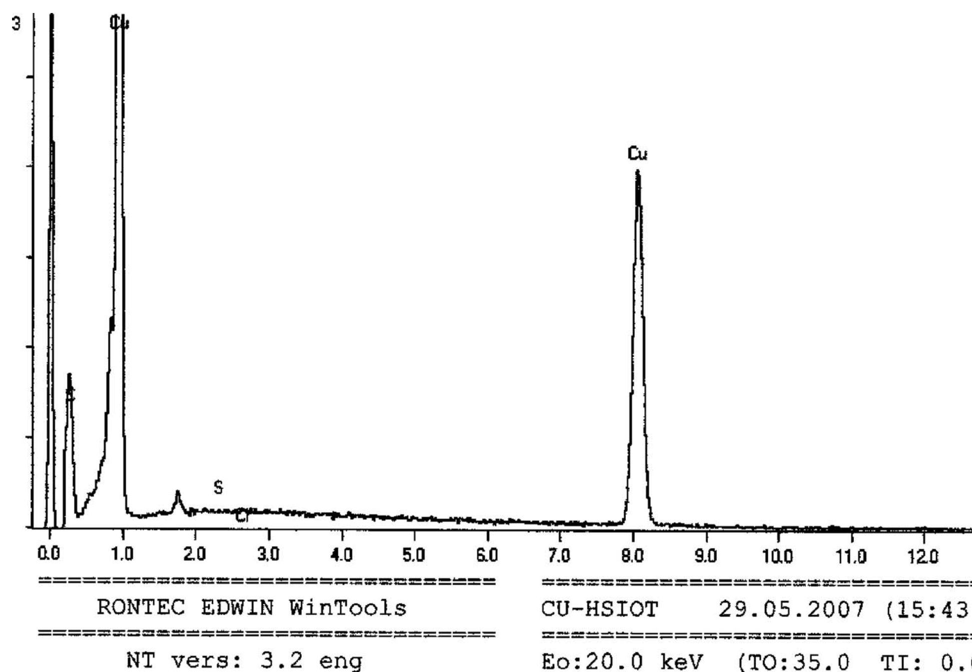

Figure 5. EDS spectrum of copper immersed for 24 h at the free-corrosion potential in 3.5% NaCl + 10^{-3} M HS^-. The spectrum was taken from a spot inside the corroded grain boundary.

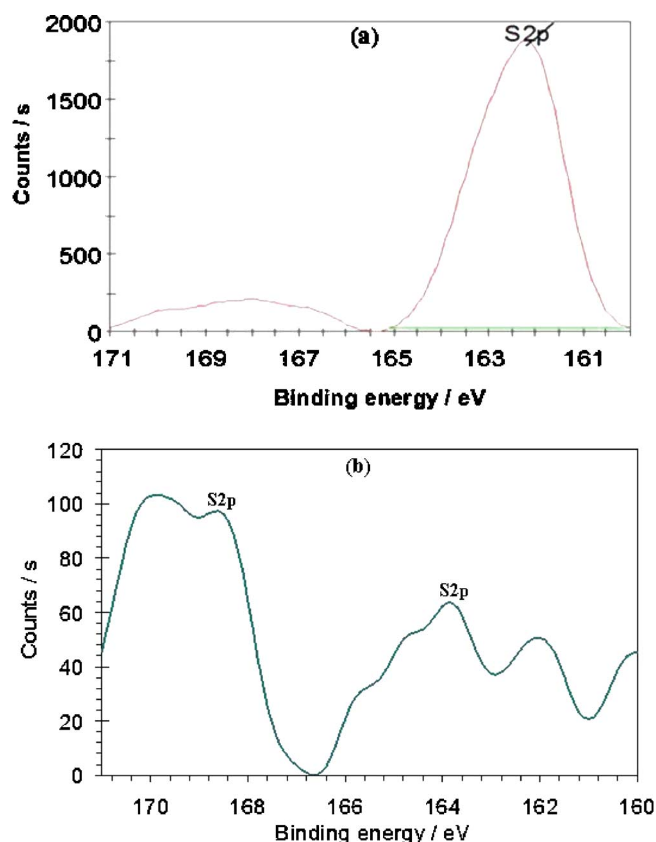

Figure 6. (Color online) XPS spectra of copper tested in 3.5% NaCl + 10^{-3} M HS^- under the following conditions: (a) immersion for 24 h at the free-corrosion potential and (b) potentiostated for 1 h at 0.0 V (Ag/AgCl).

these impurities and deficient in copper, compared to the grain surface, which is protected by a continuous layer of Cu_2O. This results in the formation of a weak Cu_2O layer on the grain boundary[3] which readily breaks down under the effect of sulfide ions.

Acknowledgments

The authors acknowledge the support of the Research Administration of Kuwait University, grant no. SC03/02 and GS01/01. They also acknowledge the use of the scanning electron microscope.

Kuwait University assisted in meeting the publication costs of this article.

References

1. G. Kear, B. D. Barker, and F. C. Walsh, *Corros. Sci.*, **46**, 109 (2004).
2. M. Chmielova, J. Siedlerova, and Z. Weiss, *Corros. Sci.*, **45**, 883 (2003).
3. X. Zhu and T. Lei, *Corros. Sci.*, **44**, 67 (2002).
4. F. Ammeloot, C. Fiaud, and E. M. M. Sutter, *Electrochim. Acta*, **44**, 2549 (1999).
5. C. Kato, B. G. Ateya, J. E. Castle, and H. W. Pickering, *J. Electrochem. Soc.*, **127**, 1890 (1980); C. Kato, J. E. Castle, and H. W. Pickering, *J. Electrochem. Soc.*, **127**, 1897 (1980).
6. Y. V. Ingelgem, A. Hubin, and J. Vereecken, *Electrochim. Acta*, **52**, 7642 (2007).
7. S. J. Yuan and S. O. Phenkonen, *Corros. Sci.*, **49**, 1276 (2007).
8. G. Mori, D. Scherer, S. Schwentenwein, and P. Warbichler, *Corros. Sci.*, **47**, 2099 (2005).
9. B. Kuznicka and K. Junik, *Corros. Sci.*, **49**, 3905 (2007).
10. Z. Yu, X. Xu, Y. Gao, and S. Liu, *Eng. Failure Anal.*, **14**, 226 (2007).
11. H. M. Shalaby and W. T. Riad, *Eng. Failure Anal.*, **15**, 38 (2008).
12. N. Ejaz and A. Tauqir, *Eng. Failure Anal.*, **13**, 452 (2006).
13. T. S. Haung and G. S. Frankel, *Corros. Sci.*, **49**, 858 (2007).
14. G. M. Ingo, T. de Caro, C. Riccucci, E. Angelini, S. Grassini, S. Balbi, P. Bernardini, D. Salvi, L. Bousselmi, A. Çilingiroglu, et al., *Appl. Phys. A: Mater. Sci. Process.*, **83**, 513 (2006).
15. D. D. Macdonald, B. C. Syrett, and S. S. Wing, *Corrosion (Houston)*, **35**, 367 (1979).
16. J. P. Gudas and H. P. Hack, *Corrosion (Houston)*, **35**, 67 (1979).
17. S. R. de Sanchez and D. J. Schiffrin, *Corros. Sci.*, **22**, 585 (1982).
18. H. Hegazy, E. A. Ashour, and B. G. Ateya, *J. Appl. Electrochem.*, **31**, 1261 (2001).
19. J. N. Alhajji and M. R. Reda, *J. Electrochem. Soc.*, **141**, 1432 (1994).
20. H. M. Shalaby, A. Al-Hashem, and K. Al-Muhanna, *Br. Corros. J., London*, **31**, 199 (1996).
21. M. Vazquez and S. R. De Sanchez, *J. Appl. Electrochem.*, **28**, 1383 (1998).
22. H. C. Xu, S. R. Seshadri, and J. A. Kelber, *J. Electrochem. Soc.*, **146**, 1762 (1999).
23. X. Xie, L. Du, L. Pan, S. Cao, M. Yan, and W. Yang, *Anti-Corros. Methods Mater.*, **54**, 34 (2007).
24. A. M. Beccaria, G. Poggi, P. Traverso, and M. Ghiazza, *Corros. Sci.*, **32**, 1263 (1991).
25. Z. Mountassir and A. Srhiri, *Corros. Sci.*, **49**, 1350 (2007).
26. J. Smith, Z. Qin, F. King, L. Werme, and D. W. Shoesmith, *Corrosion (Houston)*, **63**, 135 (2007).
27. A. Veld, *Mat. Perf.*, **45**, 52 (2006).
28. G. Huang, K. Chan, and H. P. Fang, *J. Electrochem. Soc.*, **151**, B434 (2004).
29. K. Rahmouni, N. Hajjaji, M. Keddam, A. Srhiri, and H. Takenouti, *Electrochim. Acta*, **52**, 7519 (2007).
30. C. D. Wagner, in *Practical Surface Analysis*, Vol. 1, *Auger and X-Ray Photoelectron Spectroscopy*, 2nd ed., D. Briggs and M. P. Seath, Editors, p. 595, John Wiley & Sons, New York (1990).
31. A. J. Bard, R. Parsons, and J. Jordan, *Standard Potentials in Aqueous Solutions*, p. 94, Marcel Dekker, New York (1985).
32. G. Valensi, J. V. Muylder, and M. Pourbaix, in *Atlas of Electrochemical Equilibria in Aqueous Media*, M. Pourbaix, Editor, p. 545, NACE, Houston, TX (1974).
33. U. R. Evans, *The Corrosion and Oxidation of Metals*, 2nd Supplementary Volume, p. 317, Edward Arnold, Ltd., London (1976).
34. S. Divinski, J. Ribbe, G. Schmitz, and C. Herzig, *Acta Mater.*, **55**, 3337 (2007).
35. S. Divinski, M. Lohmann, and C. Herzig, *Acta Mater.*, **49**, 249 (2001).
36. S. Divinski, M. Lohmann, and C. Herzig, *Acta Mater.*, **52**, 3973 (2004).
37. G. Erdelyi, G. Langer, J. Nyeki, L. Kover, C. Tomastik, W. S. M Werner, A. Csik, H. Stoeri, and D. L. Beke, *Thin Solid Films*, **459**, 303 (2004).
38. Y. Zhu, K. Mimura, and M. Isshiki, *Oxid. Met.*, **59**, 575 (2003).
39. G. V. Khaldeev, V. F. Knyazeva, A. B. Volyntsev, and L. V. Spikav, *Prot. Met.*, **15**, 583 (1979).